Proceedings of the
International Conference on Mechanical Engineering 2005
(ICME2005) 28- 30 December 2005, Dhaka, Bangladesh

ICME05-FL-01

STUDY OF LAMINAR FLOW THROUGH A CIRCULAR PIPE WITH SUCCESSIVE RESTRICTIONS USING A HIGHER ORDER NUMERICAL SCHEME

Debabrata Nag[1] and Amitava Datta[2]

[1]Department of Mechanical Engineering, Jadavpur University, Kolkata, India
[2]Department of Power Engineering, Jadavpur University, Kolkata, India

ABSTRACT

Flow through pipes with successive restrictions has widespread use in the fluid flow and heat transfer fields, particularly in process industries and heat exchangers. Its important applications can also be found in the field of Bio-Mechanics and Bio-Engineering particularly in the area of blood flow through stenosed artery. In presence of the restrictions, the flow field in the pipe gets completely altered, with separation of flow at the point of restrictions followed by its reattachment. The flow separation results in the formation of a recirculation zone. The effects of Reynolds number, restriction sizes and the gap between successive restrictions on the velocity field, recirculation size and the pressure drop across restrictions are investigated. It is observed that at low Reynolds number, the variation of velocity and pressure across each restriction is identical, i.e. exact repeatability can be achieved. But at high Reynolds number, this repeatability is lost and no single mathematical expression can be used to assess the flow parameters across each restriction.

Keywords: Laminar Flow, Circular Pipe, Restrictions, Recirculation.

1. INTRODUCTION

Flow through circular pipes with successive restrictions has important industrial applications in the fields of thermal and fluid engineering. Particularly its importance is noted in process industries under particular process requirement and in the design of heat –exchanging equipment, where restrictions can act as fins. The associated flow patterns developed due to the presence of such restrictions can be quite complex with the development of recirculation zones and their interactions with the confined jet. It has great influence on heat transfer effectiveness and pumping power requirement. Another application of this type flow situation can be observed in the field of Bio-Mechanics where the model can be used to study the blood flow through stenosed coronary artery for different percentage of stenosis. The importance of this type of study can be appreciated from the fact that major causes of death of human being in developed and developing countries are identified as due to the cardiovascular diseases. It is believed that the effect of interaction between the processes of oxidation, inflammatory response coupled with the phenomenon of cholesterol deposition causes the hardening of the artery followed by narrowing effect of the flow passage area results in the event of stenosis of the artery which results in reduction of blood flow and depletion of oxygen in different cells of the body. This clearly shows the importance of study of such flow hydrodynamics.

Patankar *et al.* [7-10] studied laminar and turbulent flow restricted through fins to show the effect on heat transfer. Austin *et al* [2] studied flow through Toroidal geometry to correlate Dean number with diametral pressure drop.

Fossa *et al.* [3] studied experimentally flow disturbed by thin and thick orifices placed in the two phase flow field. Oliveira and Pinho [6] studied the pressure variation in flow through sudden expansion. Such a study has important implications in the flow through restrictions as well.

Bio-mechanical applications of the present model can be found from the studies made by Siouffi *et al*.[14], Reese and Thompson [11], Zendehbudi and Moayeri [13],Tang *et al*.[12] , Anderson *et al*.[1], etc. The researchers , with the help of the computational modeling, have studied the different effects of blood flow hydrodynamics, particularly the pressure variation across the restriction and the distribution of Wall Shear Stress (WSS) ,etc in great details.In the present paper, results of a numerical study of axi-symmetric, laminar, incompressible flow through circular pipe with successive restrictions are presented. Two successive annular restrictions are considered to be fitted in the internal surface of the pipe through which the flow has been studied. The height of the restrictions equals the radius of the pipe and a separation distance of $4D_o$ is maintained between the restrictions.

2. THEORETICAL FORMULATION

The flow field is determined by solving the following equations in the computational domain using an explicit finite difference scheme.

(a)Equation of Continuity:

$$\frac{1}{r}\frac{\partial}{\partial r}(vr)+\frac{\partial u}{\partial z}=0 \qquad (1)$$

(b) Momentum Equation in z - direction :

$$\frac{\partial u}{\partial t}+\frac{\partial}{\partial r}(u\,v)+\frac{v\,u}{r}+\frac{\partial}{\partial z}(u^{2})=-\frac{1}{\rho}\frac{\partial p}{\partial z}+\nu[\frac{\partial^2 u}{\partial r^2}+\frac{1}{r}\frac{\partial u}{\partial r}+\frac{\partial^2 u}{\partial z^2}] \qquad (2)$$

(c) Momentum Equation in r- direction :

$$\frac{\partial v}{\partial t}+\frac{\partial}{r\partial r}(rv^2)+\frac{\partial}{\partial z}(uv)=-\frac{1}{\rho}\frac{\partial p}{\partial r}+\nu[\frac{\partial^2 v}{\partial z^2}+\frac{1}{r}\frac{\partial}{\partial r}(r\frac{\partial v}{\partial r})-\frac{v}{r^2}] \qquad (3)$$

The associated boundary conditions are:

$$\text{Inlet: } \frac{u(r)}{u_{avg}}=2(1-\frac{r^2}{R^2}),\ v=0 \qquad (4)$$

$$\text{Axis: Axisymmetric condition: } \frac{\partial u}{\partial r}=0,\ v=0 \qquad (5)$$

Solid Boundaries including restrictions: $u=0, v=0$ (6)

$$\text{Outlet: } \frac{\partial u}{\partial t}+u_{avg}\frac{\partial u}{\partial z}=0 \text{ and } \frac{\partial v}{\partial z}=0 \qquad (7)$$

The details of the geometry under study are shown in Fig 1 along with the computational domain which is shown as dotted line.The governing equations are discretised by a higher order upstream biased scheme – QUICK (Leonard [4]). The variable values are advanced over time step satisfying the Courant-Friedrichs –Lewy criteria and the grid Fourier number for each cell.

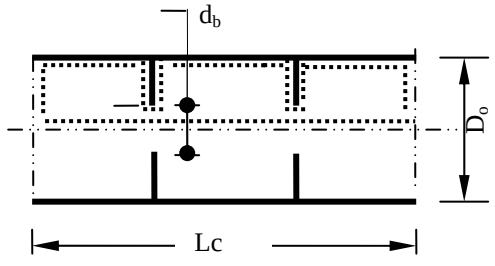

Fig 1. Physical geometry of the model under study.

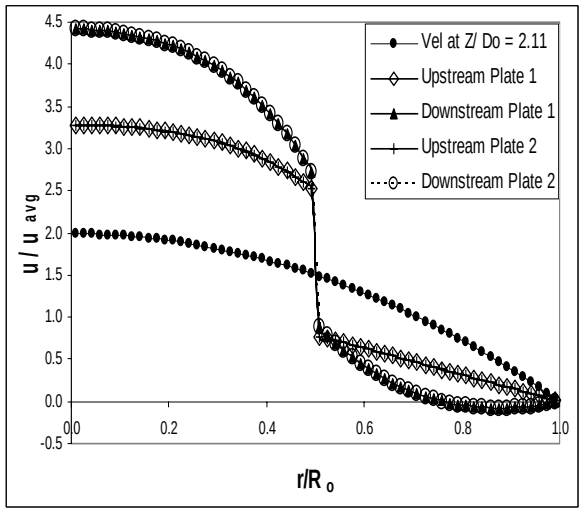

Fig 2a. Variation of axial velocity at Re=10 for D_o/d_b =2

The pressure-velocity coupling is achieved using the SOLA scheme [Hirt and Cook (1972)]. The entire code is described in the earlier work of Nag and Datta [5].

3. RESULTS AND DISCUSSION

The numerical code, after extensive testing for grid independence and validation by comparing the predictions with the results already published in the literature (Nag and Datta [5]) is applied to study the flow field with two successive restrictions for a range of Re = 10 and 150. It is observed that if the restriction size is small, no recirculation is formed at the trailing edge of the restrictions for lower Re value. However, prominent recirculation zones appear as Re increases. It is noted that, the recirculating zone after the second restriction is comparatively longer than that after the first restriction.

3.1 Velocity Variation

The fully developed parabolic velocity profile is considered at the inlet plane of the pipe. Figs 2a and 2b show the radial distributions of the axial velocity profiles at different axial positions along the length of the pipe for two different Reynolds numbers (Re= 10 and 150). The parabolic profile is maintained for some length before the first restriction is approached in both the cases, as are shown by the velocity profiles at $Z/.D_o$ = 2.11 (Figs 2a and 2b). When the first restriction is reached, the fluid flow gets obstructed near the periphery and tends to converge towards the core. As a result, the axial velocity near the core increases. Fig 2a shows that upstream to the first restriction a parabolic profile with much higher centerline value is observed to exist up to a radial position equal to the passage opening and then a sudden jump in velocity occurs to a much lower value. From this point up to the wall the axial velocity falls almost linearly to the zero value. Just downstream to the first restriction, the axial velocity at the core gets further accelerated maintaining a near parabolic shape. A recirculation zone with negative axial velocity is now observed at the periphery. It is important to observe from the velocity distributions across the first and second restrictions in this case (Fig 2a) that they are exactly identical. This proves that for a low Re = 10 and with present size of the

restriction and the separation between them, the flow repeats itself across every restriction.

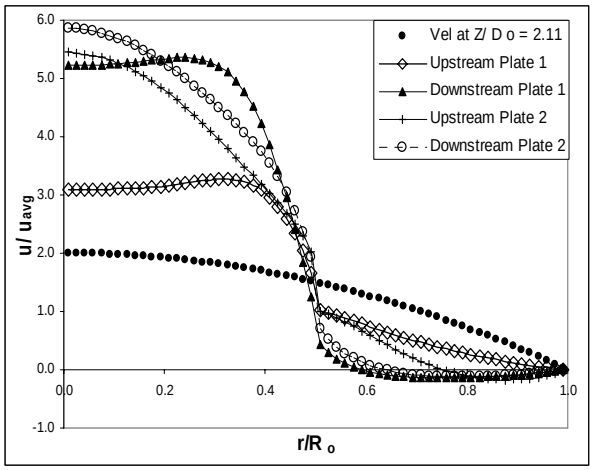

Fig 2b. Variation of axial velocity at Re=150 for D_o/d_b=2

Fig 2b shows the results at a higher Re=150. Differences are now observed in the velocity profiles across the two restrictions. Upstream to the first restriction the axial velocity profile again is distorted from the original parabolic shape. The velocity profile in the core and up to the radius of the passage opening maintains a parabolic shape with much higher center line value. However, unlike in the previous case, there is no sudden jump in the axial velocity. Instead, the velocity gradually reduce up to r / R_o = 0.5 and then falls linearly to zero. Down stream to the first restriction, the maximum axial velocity shifts to an off-axis location and a much wider wall recirculation zone is observed. The shapes of the velocity profiles upstream and downstream to the second restriction are somewhat qualitatively similar to those around the first restriction but differ quantitatively from one another. Particularly important is that the velocity near the periphery upstream to the second restriction is still negative over a certain radial position, showing that the recirculation zone down stream to the first restriction fills the entire space between the two restrictions. These results indicate for a particular size and spacing of the restrictions, the velocity distributions do not repeat themselves across every restriction beyond a critical Reynolds number.

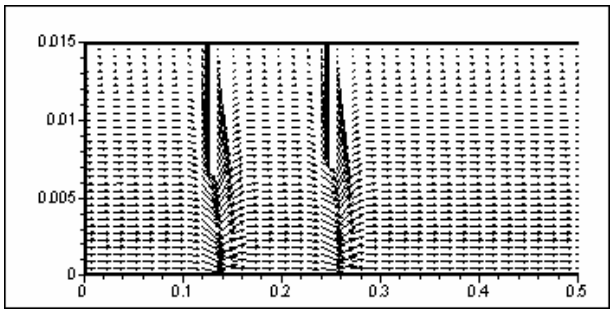

Fig 3a. Velocity plot at Re=10 for D_o/d_b=2

Fig 3a and 3b show the velocity vector plots for the conditions represented by Re = 10 and Re =150 for the case when Do/db = 2.

The Fig 3a shows the partial flow field and the recirculation zones created by the obstructions placed at a distance of $4D_o$ apart. At this small value of the Reynolds number, the reicirculation zones are formed downstream of the each restriction but the recirulation size is too small to engulf the inter-spacing distance between the restrictions. Obviously, at such a small Reynolds number, the exact repeatability of the flow structure and hence the velocity variations etc, can repeat itself should there be a periodic arrangement of the restrictions along the stream-wise direction.

A distinctive difference in pattern of the velocity vector plot can be observed in the Fig 3b where conditions are depicted for a higher Reynolds number for the same geometric arrangement of the flow passage.

In this case, again the recirculation zones are formed as usual at the downstream portion of the each restriction placed at a distance of $4D_o$ apart. As the flow velocity increases with the increase of the inlet Reynolds number, the recirculation zones also grow bigger and one recirculation zone covers completely the interspacing distance between the two successive restrictions. Consequently, each flow field separated by the compartment zone created by the restriction gets influenced by the previous flow filed. Obviously, in such cases, the exact repeatability of the flow structure as well as the velocity filed, etc are lost in the cases of the periodic arrangement of the restrictions placed along the stream –wise direction in the flow field.

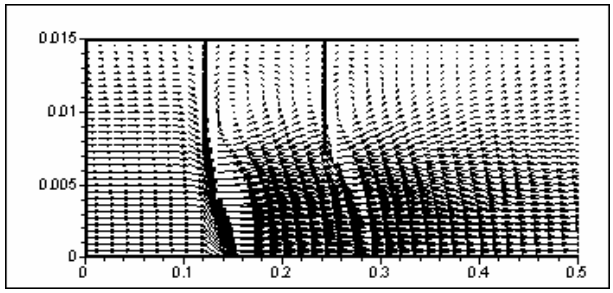

Fig 3b. Velocity plot at Re=10 for D_o/d_b=2

3.2 Pressure Variation

Progressive pressure drop along the full pipe length, expressed in terms of pressure drop coefficient C_p , are shown in Figs 4a and 4b for Re= 10 and 150, respectively. It is observed from the fig 4a that the pressure drop across each of the restrictions is of the same order for low Re. It is also seen from the figure that at each restriction the pressure initially falls and subsequently some pressure recovery takes place as the flow adjusts itself. The equal velocity change across each restriction at low Re found earlier is corroborated by the pressure distribution. Fig 4a also shows the theoretical pressure distribution line for fully developed pipe flow. It is found that at some distance downstream to the first restriction, the predicted pressure drop line with restrictions becomes parallel with the theoretical line only with a lateral shift. This shows that the flow achieves its fully developed characteristics after getting distorted at the first restriction and before the second restriction is reached.

The situation is not so with higher Re as depicted in Fig 4b. Here it is observed that a large drop in pressure occurs across the first restriction and the pressure recovery still continues when the second restriction is reached. The pressure upstream to the second restriction is much low as the recirculating eddy extends up to this point. Further drop in pressure occurs across the second restriction plate, but this drop is much smaller than that across the first restriction. The pressure recovery again occurs downstream to the second restriction and finally the C_p line becomes parallel to the theoretical line, indicating that the fully developed pipe flow is reached.

A variation of wall shear stress at the pipe surface is studied along the pipe length and expressed in terms of friction factor (f) for two different Re (Figs 5a and 5b). the theoretical value of 'f ' for fully developed pipe flow given by Darcy-Weisbach equation f = 64/Re is also drawn for the sake of comparison. Negative value of 'f' indicates reversal of flow at the wall. Fig 5a clearly shows identical changes in 'f' across each restriction and it further shows that the sizes of the recirculating eddy with negative velocity adjacent to the wall across each restriction are small.

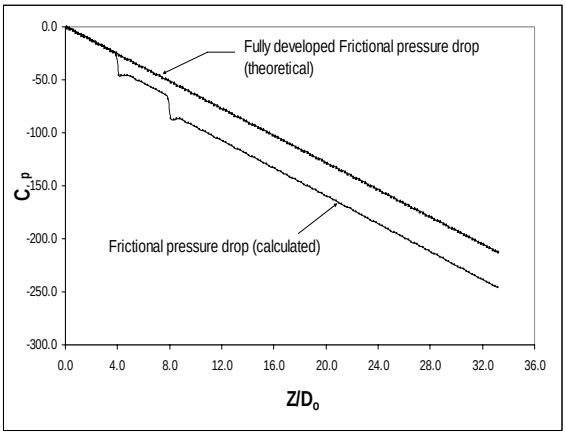

Fig 4a. Variation of Pressure drop coefficient at Re =10 for D_o/d_b =2

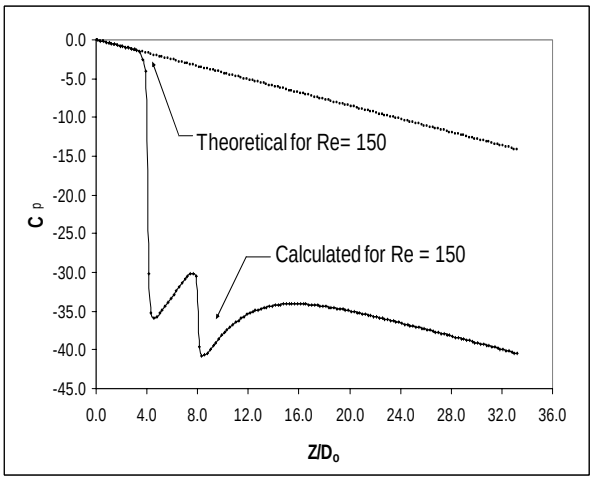

Fig 4b. Variation of Pressure drop coefficient at Re= 150 D_o/d_b = 2

Fig 5b, however, indicates that 'f' is negative in the entire interspace, showing the existence of the recirculating eddy there. The repeatability in the variation of 'f' across the restrictions is clearly lost in this case.

4. CONCLUSIONS

A numerical study of laminar, incompressible flow through a circular pipe with two successive annular restrictions is studied. The velocity and pressure variations across the length of the pipe and the variation of the friction factor are studied with particular interest to focus on the changes across the restrictions. It is found that, at low Re, the variations across the first restriction exactly repeats themselves across the second. This repeatability is lost at high Re. Beyond a critical Re, based upon the restriction size and their interspacing the recirculating eddy downstream to the first restriction extends up to the second one. Under that condition, the pressure drop across the first restriction far exceeds that across the second and the wall friction factor remains negative throughout the interspacing. In such a situation, no single mathematical expression for pressure drop can be used for each restriction.

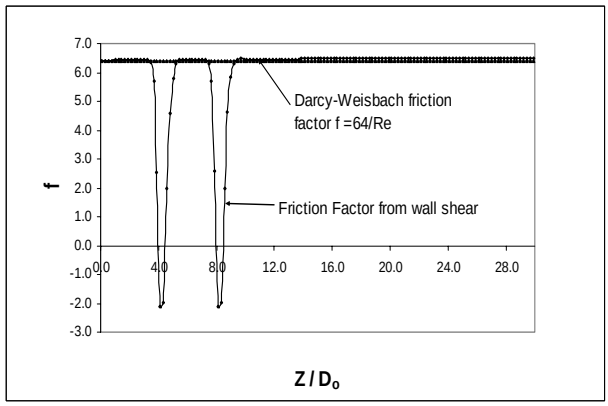

Fig 5a.Variation of friction factor at Re=10 for D_o/d_b=2

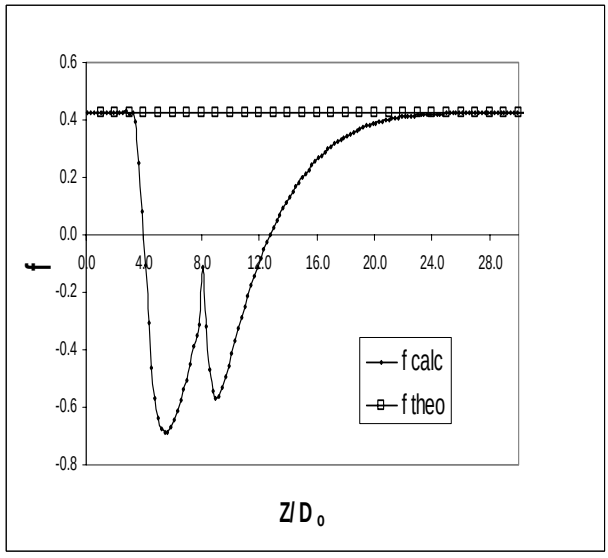

Fig 5b.Variation of friction factor at Re= 150, D_o/d_b= 2

5. REFERENCES

1. Anderson, H.I., Halden, R., Golmasker, T., 2000, "Effects of Surface Irreuglarities on Flow Resistance in differently shaped Arterial Stenosis", J. Bio-Mechanics, Vol 33, pp.1257-1262.
2. Austin, L., Seader, J., 1972, "Fully Developed Viscous Flow in Coiled Circular Pipes", AIChE J., Vol. 19, Issue 1, pp. 85-94.
3. Fossa , M., Guglielmini, M., 2002, "Pressure Drop and Void Fraction Profiles during Horizontal Flow through Thin and Thick Orifices", Exp.Thermal and Fluid Sc. J. Vol. 26, pp. 513-523.
4. Leonard, B.P., 1979, "A Stable and Accurate Convective Modeling Procedure based on Quadratic Upstream Interpolation", Comput. Meth Appl. Mech. Engg , Vol. 19, pp. 59.
5. Nag , D., Datta , A., 2004 , " A Study on Laminar Flow through Confined Geometries with Sudden Expansion using a Higher Order Numerical Scheme" , *Proc. 31st Nat. Conf. On Fluid Mech. and Fluid Power* , India, Vol. 1, pp. 164 – 171.
6. Oliveira, P.J.,Pinho, F.T., 1997, " Pressure Drop Coefficient of Laminar Newtonian Flow in Axisymmetric Sudden Expansions",Int. J. Heat and Fluid Flow, Vol. 18, pp. 518-529.
7. Patankar et al., 1977, "Fully Developed Flow and Heat Transfer in Ducts having Streamwise- Periodic Variations of Cross Sectional Area", J. Heat Transfer., Vol. 99, pp. 180.
8. Patankar et al., 1979, "Analysis of Turbulent Flow and Heat Transfer in Internally Finned Tubes and Annuli", J. Heat Transfer, Vol. 101, pp. 29.
9. Patankar , S.V., Prakash , C. ,1981, " An Analysis of the Effect of Plate Thickness on Laminar Flow and Heat Transfer in Interrupted-Plate Passages", Int. J. Heat and Mass Transfer, Vol.24, Issue 11, pp. 1801-1810.
10. Patankar , S.V., Rowley, G. J. ,1984, " Analysis of Laminar Flow and Heat Transfer in Tubes with Internal Circumferential Fins", Int. J. Heat and Mass Transfer, Vol.27, Issue 4, pp. 553-560.
11. Reese, M.J., Thompson, D.S., 1998, "Shear Stress in Arterial Stenoses : A Momentum-Integral Method", J. Bio-Mechanics, Vol.31, pp. 1051-1057.
12. Tang, D., Yang, J., Yang, C., Ku, D.N., 1999, "A Non- Linear Axisymmetric Model with Fluid-Wall Interaction for Steady Viscous Flow in Stenotic Elastic Tubes", J. Bio-Mechanical Engineering, Vol. 121, pp. 494-501.
13. Zendehbudi, G.R.,Moayeri, M.S.,1999, "Comparison of Physiological and Simple Pulsatile Flow through Stenosed Arteries", J. Bio-Mechanics, Vol.32, pp. 959-965.

6. NOMENCLATURE

Symbol	Meaning	Unit
C_p	Coefficient of Pressure ($=\partial p \ / \ p_{dyn}$)	-
d_b	Diameters of Restrictions	(m)
D_o	Outer Diameter of Pipe	(m)
L_c	Computational Length	(m)
f_{calc}	Friction Factor from Wall Shear Stress ($=8\tau_w \ / \ \rho u^2{}_{avg}$)	-
f_{theo}	Friction Factor from Darcy-Weisbach Equation (= 64/Re)	-
p	Thermodynamic Fluid Pressure (abs.)	(Pa)
p_∞	Upstream Fluid Pressure	(Pa)
p_{dyn}	Dynamic Pressure ($=\frac{1}{2} \rho \ u^2{}_{avg}$)	(Pa)
∂p	Pressure Drop ($= p - p_\infty$)	(Pa)
r	Radial Distance	(m)
r_o	Outer Radius of Pipe	(m)
Re	Reynolds Number ($=\rho \ u \ d_o / \mu$)	-
t	Time	(sec)
u_{avg}	Mean Axial Velocity	(m/s)
u	Axial Velocity	(m/s)
v	Radial Velocity	(m/s)
z	Axial Distance	(m)
ρ	Density of Fluid	(Kg/ m^3)
μ	Dynamic Coefficient of Viscosity	(Pa.s)
τ_w	Wall Shear Stress	(Pa)